

# Limitations to the short term frequency stability in a compact cold atom clock

Stephane Tremine\*, Stephane Guerandel\*, David Holleville\*, Jerome Delporte†, Noel Dimarcq\* and Andre Clairon\*

\*LNE-SYRTE, Observatoire de Paris, Paris, France

Email: stephane.tremine@obspm.fr

†CNES, Toulouse, France

**Abstract**—The HORACE device is a compact cold atom clock where about  $10^8$  cesium atoms are laser cooled at a few  $\mu\text{K}$ , then interrogated and detected directly in a  $20 \text{ cm}^3$  spherical microwave cavity. The optimization of the short term stability with the cooling and interrogation durations is presented, leading to an estimation of the Allan deviation of  $\sigma_y(\tau) = 1 \cdot 10^{-13} \tau^{-1/2}$  on earth and  $\sigma_y(\tau) = 7 \cdot 10^{-14} \tau^{-1/2}$  in space. The quantum projection noise, the Dicks effect and the detection laser noises are taken into account. The calculations are based on a preliminary model for the recapture of cold atoms, in reasonable agreement with measurements.

## I. INTRODUCTION

The aim of the HORACE project is to realize an atomic clock for the future generations of GALILEO satellites, for which the required short term frequency stability is about  $10^{-12}$  at 1 s. In the past ten years, frequency standards based on atomic fountains have been developed and reached short term stabilities in the range of  $10^{-14}$  at 1s. Today we propose to realize a compact cold atomic clock using laser cooling techniques with all the clock steps in the same region, in order to reach ultimately a short term stability in the range of  $10^{-13}$  at 1s under micro-gravity.

The first part of this paper is dedicated to the description of the experiment and the first results. In the second part, we present a simple model for the recapture of cold atoms in our clock. Then, we use this model to predict the short term frequency stability and compare the operation on earth and in space.

## II. THE DEVICE AND THE FIRST RESULTS

### A. The physics package

A cesium vapor is contained in a quartz bulb of 33 mm diameter (see Fig. 1), in which the vacuum is  $4 \cdot 10^{-9}$  Torr. The quartz bulb is surrounded by a spherical copper cavity which has two functions. The first one is to perform the cooling of the cesium atoms. For this purpose, the cavity is optically polished in order to build an isotropic light field in which about  $10^8$  atoms with temperatures as low as  $2 \mu\text{K}$  can be trapped. The cooling light is carried to the cavity by 6 multimode optical fibers. The second function of this cavity is to be a microwave resonator for the clock interrogation and is fed by evanescent coupling with two antennas. Obviously, the volume of the cavity (40 mm) is defined by the interrogation wavelength (32.6 mm for cesium).

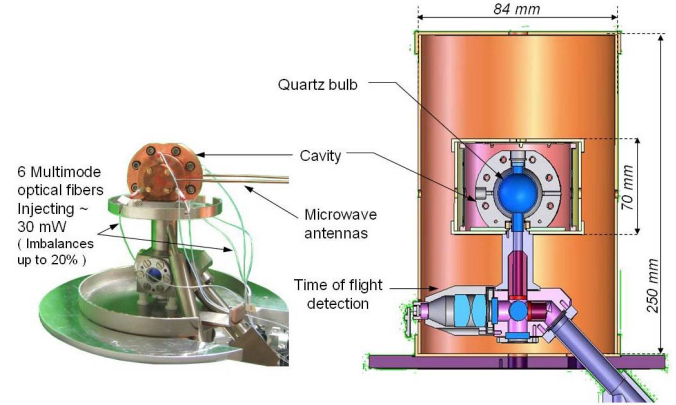


Fig. 1. Views of the physics package. On the left : the cavity set around the quartz bulb and fed with the cooling light by six fibers, and with the microwave via two antennas. On the right : cross section of the whole device.

At the bottom of the device, a time of flight detection region is used to measure the number of atoms in the cloud and their temperature. This part is dedicated to diagnostics only, and is not used in the clock sequence.

Finally, two magnetic shields enclose the cavity region, realizing a global attenuation factor of about 7000. Presently the volume of the physics package is about 5 liters, but without the diagnostic part, it finally could be reduced to 1 or 2 liters.

### B. The clock working process

One cycle first consists in laser cooling the atoms from a cesium vapor. Then, the cooling light is switched off and the cloud, in thermal expansion, starts to fall under gravity. The Ramsey interrogation is then performed in the microwave cavity before the atomic populations are detected by absorption of a vertical laser beam. In the next cycle, previously cooled atoms are partly recaptured. Thus, the cooling time can be reduced at the benefit of the interrogation time.

### C. The first results

Spectroscopic results obtained on our device are presented in Fig. 2. The cooling, preparation and interrogation phases have been validated inside the cavity [1] by a time of flight detection. The fringes presented in Fig. 2 have been obtained by detecting only one population. The signal to noise ratio is

about 200 in 1 Hz bandwidth, and is limited by the number of cold atoms fluctuations. Our narrowest fringes have a linewidth of 9 Hz, and are obtained for a 50 ms Ramsey interrogation time. The contrast is 85%.

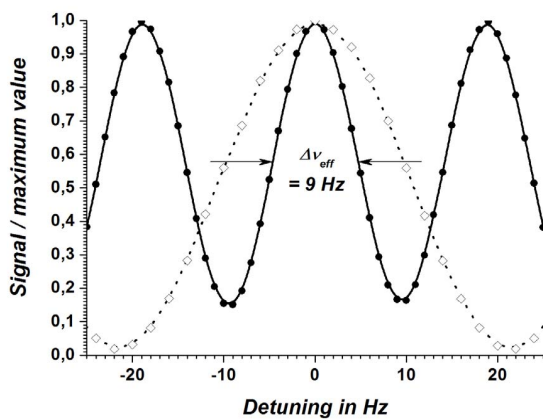


Fig. 2. Experimental Ramsey fringes of the clock transition. (··· ◊···) Interrogation time set to 20 ms. The full width at half of the peak-to-valley signal is 22 Hz. The contrast is 98%. (—●—) Interrogation time set to 50 ms. FWHM  $\sim$  9 Hz. The contrast is 85%.

These results are not sufficient to reach a frequency stability of a few  $10^{-13}$  at 1 s. Further noise rejection will be implemented in the sequence with population normalization in order to reach a SNR of about 1000 in 1 Hz bandwidth.

### III. SHORT TERM FREQUENCY STABILITY

The short term stability is given by Eq. 1 which consists in the quadratic sum of the quantum projection noise [2], the detection noise [3] [4] [5] and the local oscillator phase noise [6] [7].

$$\sigma_y^2(\tau) = \sigma_{y,QPN}^2(\tau) + \sigma_{y,detection}^2(\tau) + \sigma_{y,Dick}^2(\tau) \quad (1)$$

The quantum projection noise and the detection noise (III-C) are two limitations that depend on the number of the detected atoms (III-B). This number is subordinate to the cooling duration and the interrogation duration through the recapture process (III-A). The local oscillator phase noise (III-D) directly depends on these two durations through the cyclic ratio.

The purpose of the next section is to minimize the limitations by adjusting the two durations.

#### A. Cold atoms recapture

[8] [9] A clock sequence alternates cooling phases with dead times (see Fig. 3), during which we carry out the interrogation and the detection.

We gain atoms during the cooling phases, and loose atoms during the dead times. After a few cycles, balance is reached leading to a stationary number of atoms inside the cavity. During the dead time, the loss of atoms depends on gravity,

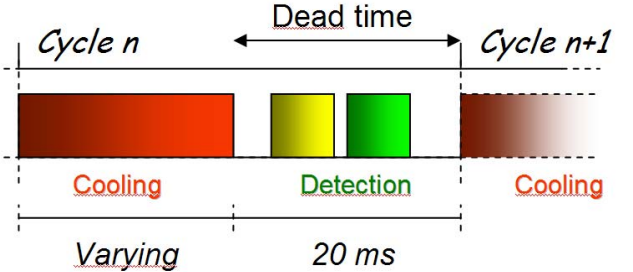


Fig. 3. Typical clock cycle. The sum of the detection and the interrogation phases is called a "dead time" for the recapture. It is set to 20 ms for the measurements presented in Fig. 5.

the thermal expansion of the cloud and the collisions with the cesium vapor (see Fig. 4). Moreover, the detection sequence can increase this loss.

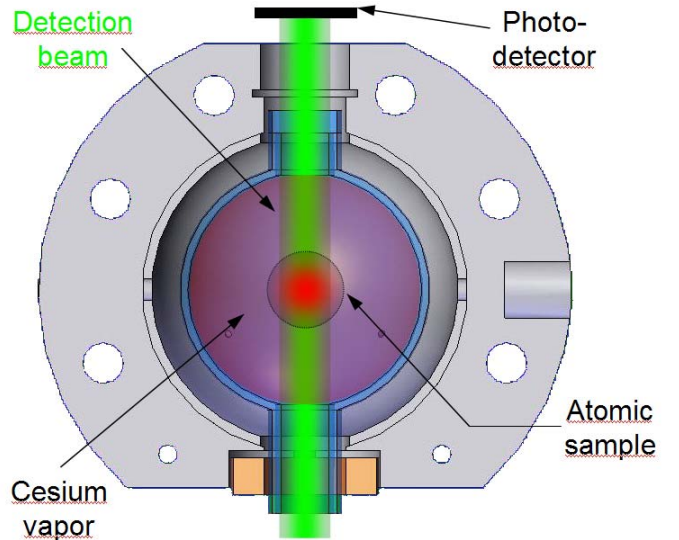


Fig. 4. Detection scheme.

In Fig. 5, we present measurements of the number of atoms reached after  $n$  cycles, for a dead time set to 20 ms, and for different values of the cooling duration. We can observe that a stationary number of atoms is reached after about ten cycles. For a long enough cooling phase, the maximum number of trapped atoms is  $3 \times 10^8$ . Looking at the curve pointed out by the arrow, corresponding to 30 ms cooling time, we can see that about a third of the maximum value is reached, i.e.  $10^8$  atoms.

We need to be able to predict this stationary number for any cooling duration and for any dead time.

#### B. Number of detected atoms

In this subsection, we present a simple model for the recapture of cold atoms. The number of atoms trapped in the molasses after a time  $T_{cool}$  is given by Eq. 2, and the loss of atoms during the dead time  $T_{dead}$  (interrogation time + detection time) is given by Eq. 3.

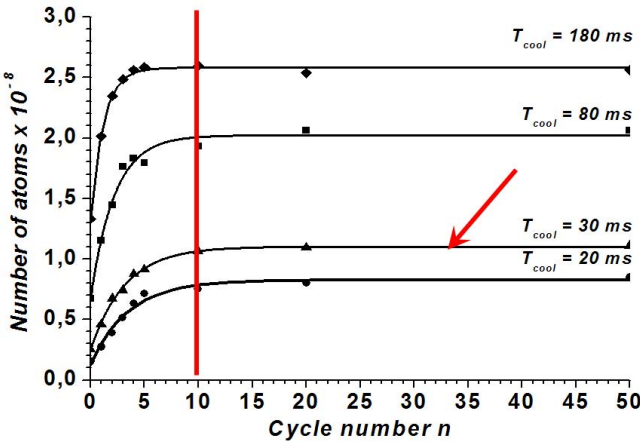


Fig. 5. Experimental measurements of the atom number reached after "n" recapture cycles versus "n", and for different cooling durations "Tcool". A stationary number (given by eq. 5) is reached after about 10 cycles.

$$N_{gain}(t) = N_\infty \times (1 - a) \quad \text{with} \quad a = e^{-T_{cool}/\tau_C} \quad (2)$$

$$N_{loss}(t) = N_0 \times b \quad \text{with} \quad b = e^{-T_{dead}/\tau_P} \times F[T_{dead}, T, g] \times (1 - 0.08) \quad (3)$$

$N_\infty$  is the maximum number of atoms than can be trapped (3  $10^8$  in our case).  $\tau_C$  is the loading time and  $1/\tau_P$ , the loss rate.  $F[T_{dead}, T, g]$  takes the atomic fraction lost during the "dead time" into account, and depends on the temperature of the cloud  $T$  and the gravity  $g$ . Its value is given by a Monte-Carlo simulation where the trapping volume is defined by the quartz bulb itself. The last term "(1 - 0.08)" gives the losses due to the detection sequence [1], where 8% of the atoms are cleared out for the normalization (16% of the atoms are contained in the  $m_F = 0$  Zeeman sublevel. One half makes the transition during a cycle and are cleared out.). Moreover only the atoms that are in the detection beam, are considered. One can now calculate the number of atoms at any step of the clock cycle.

At the end of the first cooling phase, the number of atoms (noted  $N_0$ ) is given by Eq. 2. Then, for the next cycle we obtain Eq. 4, where  $\Delta N_1$  is the gain of atoms due to the second cooling phase.

$$N_1 = N_0 \times b + \Delta N_1 = N_\infty \times (1 - a) \times [1 + a.b] \quad (4)$$

One can easily find that the stationary number of atoms  $N_{stat}$  reached after few cycles is given by Eq. 5 (result of a geometrical suite with a ratio  $a.b$ ).

$$N_{stat} = N_\infty \times \frac{1 - a}{1 - a.b} \quad (5)$$

Calculations of  $N_{stat}$  have been performed varying  $T_{cool}$  and  $T_{dead}$  from 0 to 100 ms (In fact,  $T_{dead} \geq 10$  ms when

given by the detection duration only). The results are presented in Fig. 6. The maximum value reached for long cooling phases and short interrogation durations, is about  $10^7$  atoms. The fast decrease around 60 ms is due to the atomic sample leaving the cavity.

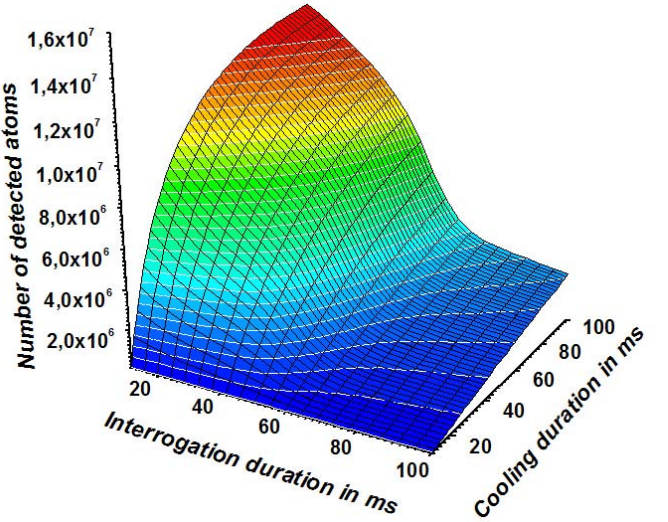


Fig. 6. Calculation of the detected atom number (only atoms contained in the vertical beam) versus the cooling and interrogation durations.

We are now able to calculate the short term stability limitations for any cooling and interrogation times.

#### C. Detection laser noise

A laser passes through a cesium vapor and the cold atomic sample before being detected on a photodiode (Fig. 4). With a laser intensity of  $I_{sat}/10$  and a detuning set to  $\delta \sim -\Gamma/2$  (which will maximize the sensitivity to laser noises), the absorption levels seen by the detector are presented in Fig. 7.

Without any absorption, the transmitted intensity is given by the dashed line. The cesium vapor (considering the density used in our device) absorbs about 50% of the light and the cold atoms, about 15%. Three detection pulses will be generated to measure successively the population of the level  $F = 3$ , the cesium vapor background, and the population of the level  $F = 4$ .

Two operations in the time domain consisting in the background subtraction and the probability calculation will filter fluctuations of the laser frequency and intensity [1]. With spectral density fluctuations of  $S_y(f) \sim 2 \cdot 10^{-26} \text{ Hz}^{-1}$  for the frequency, and  $S_{\delta I/I}(f) \sim 3 \cdot 10^{-9}/f$  for the intensity (corresponding to a laser externally locked to a cesium line and intensity locked by an acousto optic modulator), we can calculate the contributions of the "background subtraction" and the "transition probability calculation". They are respectively  $2.8 \cdot 10^{-14}$  and  $3.6 \cdot 10^{-14}$ . Those contributions include the laser intensity fluctuations at the detector, and the frequency to amplitude conversion noise due to both cold and thermal cesium atoms separately.

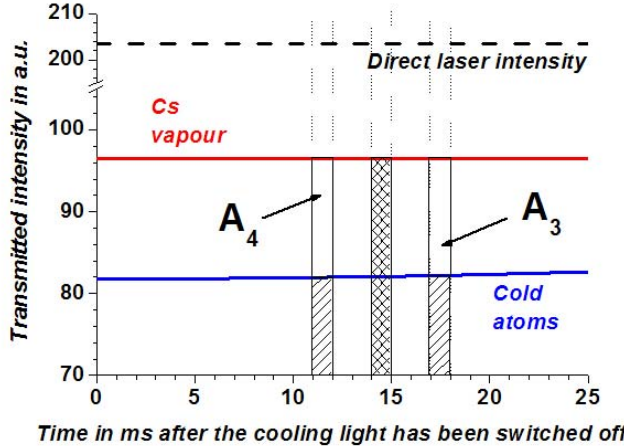


Fig. 7. Transmitted laser intensity seen by the detector after absorption by the cesium vapor and the cold atomic sample, versus the elapsed time after the cooling light has been switched off. The detection sequence used for the transition probability calculation is presented.

The result is a limitation by the detection noise at the level  $5 \cdot 10^{-14}$ . This number is obtained with the phase durations that optimize the sequence (III-E.1).

#### D. Preliminary noise budget and Dick effect

If we only sum the quantum projection noise and the detection noise for all the data presented in Fig. 6, we find an optimum for a cooling time of 45 ms and an interrogation time of 35 ms. The corresponding limitation is  $\sigma_y(1s) \sim 8 \cdot 10^{-14}$ . The whole cycle duration is  $T_{cycle} \sim 90$  ms. Consequently, if we want to minimize the contribution of the local oscillator phase noise to the budget, we have to look for an optimized one in the frequency range of 10 Hz. In Fig. 8 we give the spectral density of frequency noise for such an oscillator (the one called "HORACE Earth") versus the cycle frequency. In terms of phase noise (most commonly used), the dashed line would be given by Eq. 6 with  $A = -84$ ,  $B = -120$  and  $C = -130$  (in dB $\text{rad}^2\text{Hz}^{-1}$ ).

$$S_\phi(f) = \frac{A}{f^3} + \frac{B}{f} + C \quad (6)$$

#### E. Calculated performances

1) On Earth: If we now add up all the contributions, including the local oscillator phase noise, we finally obtain the data presented in Fig. 9. The corresponding optimum (indicated by the arrow) is obtained for a cooling duration of 25 ms (Fig. 10) and an interrogation of 40 ms (Fig. 11).

The short term stability improves rapidly in the first part of the Fig. 10 as the number of trapped atoms increases (improvement of the signal to noise ratio). In the second part, the short term stability degrades since the cyclic ratio decreases. Indeed, the cycle duration becomes to high compared to the gain in atoms in this region.

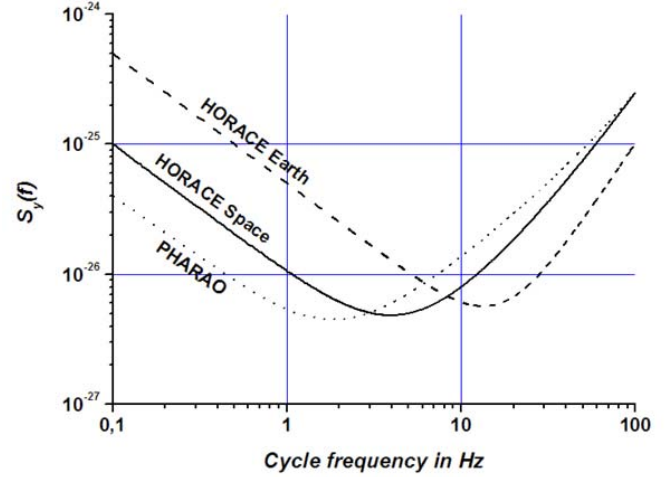


Fig. 8. Calculated spectral density of frequency noise for different local oscillator versus the cycle frequency. (· · ·) Existing local oscillator used in the PHARAO project [10]. (—) Optimized local oscillator for the HORACE project on Earth. (—) Optimized local oscillator for the HORACE project in Space.

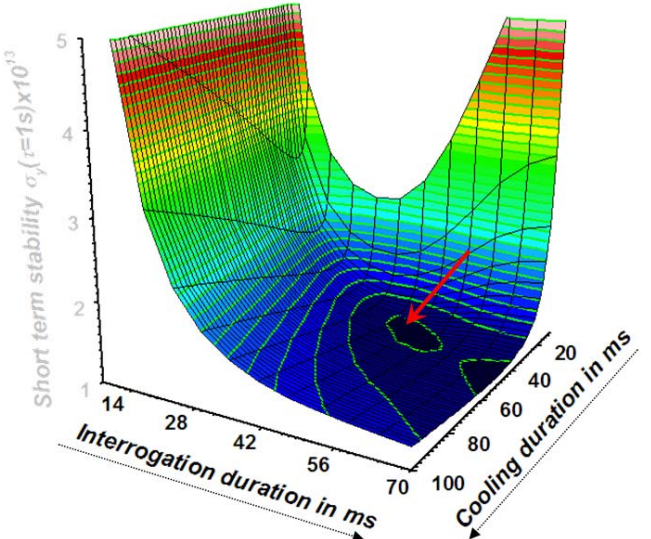


Fig. 9. Calculated short term stability on Earth versus the cooling and interrogation durations. The arrow indicate the optimization point where  $T_{cool} = 25$  ms and  $T_i = 40$  ms. Two cross section of this graph are respectively presented on Fig. 10 for the cooling duration and Fig. 11 for the interrogation duration.

The dependance on the short term stability (Fig. 11) improves for low interrogation duration as the linewidth does, until the loss of atoms between two cooling phases becomes to high (second part). The vertical line drawn on the graph at 60 ms indicates the moment when the atoms leave the cavity. Consequently, the calculation does not make sens after this line.

The corresponding short term stability limitation is  $\sigma_y(\tau) \sim 1 \cdot 10^{-13} \tau^{-1/2}$ , where all the contributions are in the same

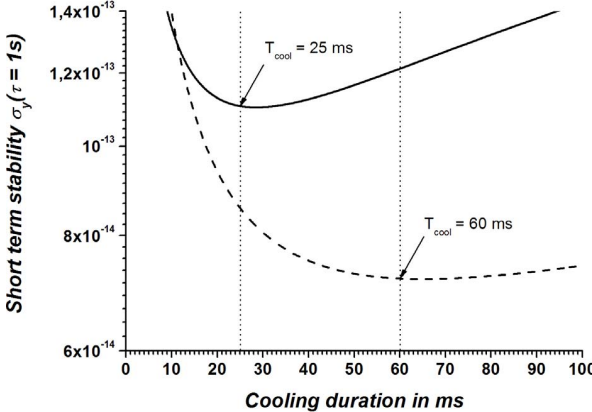


Fig. 10. Calculated short term stability on earth (—) and in space (---) versus the cooling duration (extracted from Fig. 9 on earth).

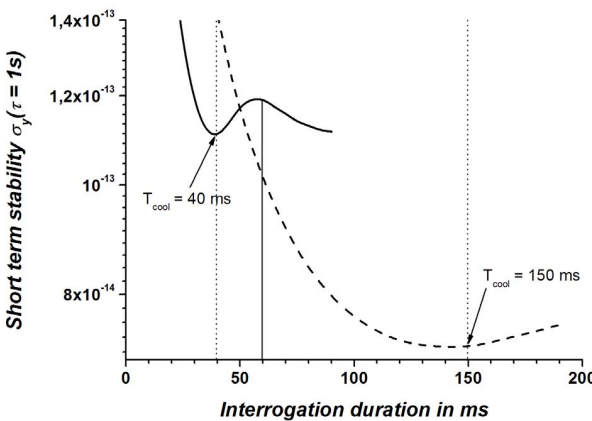


Fig. 11. Calculated short term stability on earth (—) and in space (---) versus the interrogation duration (extracted from Fig. 9 on earth).

range (see Tab. I).

2) *In space*: If we now proceed in the same way but in a micro-gravity environment, which will increase the detected atoms number for longer interrogation durations, we obtain the data presented in Fig. 12. These results include the choice of an appropriate local oscillator ( $A = -93$ ,  $B = -120$  and  $C = -120$  in Eq. 6), here optimized for a 5 Hz cycle frequency (see Fig. 8 - oscillator "HORACE Space"). The optimization of the short term stability is obtained for a cooling time of 60 ms and an interrogation duration of 150 ms. The expected stability is  $\sigma_y(\tau) \sim 7 \cdot 10^{-14} \tau^{-1/2}$  (see Tab. I).

We don't have a great improvement of the performances in space. This is due to the cloud temperature ( $35 \mu\text{K}$ ). A solution would be to have a complete Sisyphus phase leading to  $T \sim 2 \mu\text{K}$  [11]. At the present time, this phase is too long and leads to less atoms (about a third), but it needs to be studied further. Indeed, in this case we would have much longer cooling phases (Sisyphus phase added), but it

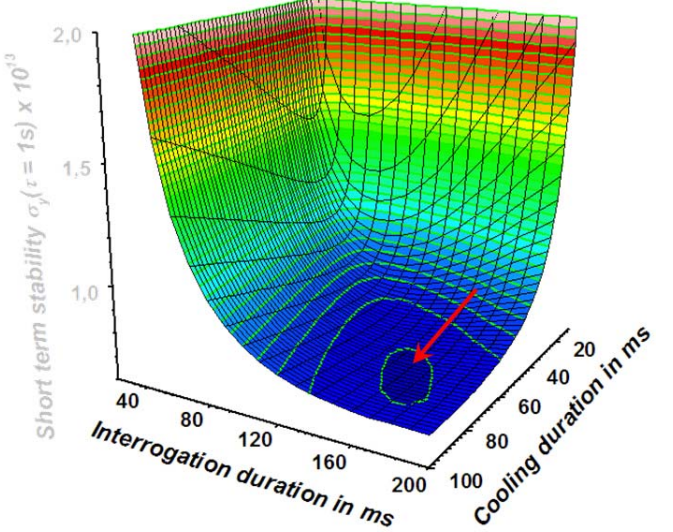


Fig. 12. Calculated short term stability in Space versus the cooling and interrogation durations. The arrow indicate the optimization point where  $T_{cool} = 60$  ms and  $T_i = 150$  ms.

	Earth	Space
Quantum projection noise	$8 \cdot 10^{-14}$	$5 \cdot 10^{-14}$
Detection noise	$5 \cdot 10^{-14}$	$3 \cdot 10^{-14}$
Local oscillator phase noise	$7 \cdot 10^{-14}$	$5 \cdot 10^{-14}$
Total $\sigma_y(1s)$	$1 \cdot 10^{-13}$	$7 \cdot 10^{-14}$

TABLE I

Contributions to the short term stability of the quantum projection noise, the detection noise and the local oscillator phase noise, on earth and in space.

would allow longer interrogation time. Consequently, a more interesting compromise than the one presented in Tab. I and II, could be reached in space.

#### IV. CONCLUSION

Using a simple model for the recapture of cold atoms, we have been able to predict the performances of the clock working on earth or in space (a summary is presented in Tab. II). The gain in a micro-gravity environment is not as big as we could expect, but the recapture using a sample at  $2 \mu\text{K}$  has to be studied. Nevertheless, the results presented in Tab. II have to be taken with caution. Indeed, the model given for the recapture in subsection III-A overestimates the number of atoms for small cooling durations. In these calculations, we have considered losses (during dead times) independent of the cycle number. In fact, it has been observed that the cloud's center of gravity goes down until the stationary state is reached, which induces different losses for each cycle. These corrections will be added to build a new model.

#### ACKNOWLEDGMENT

This work is supported in part by CNES. S. Tremine is grateful to CNES and SODERN for providing research studentship.

	Earth	Space
Linewidth	12 Hz	3 Hz
Cycle duration	75 ms	220 ms
Detected atoms	$2.5 \cdot 10^6$	$1.3 \cdot 10^6$
$S/N_{1\text{ Hz}}$	1200	750
$\sigma_y(1s)$	$1 \cdot 10^{-13}$	$7 \cdot 10^{-14}$

TABLE II

Summary of the calculated performances on earth and in space.

## REFERENCES

- [1] S. Tremine, S. Guerandel, D. Holleville, N. Dimarck, J. Delporte, A. Clairon, *Short term stability limitations in a compact cold atom clock*, In Proc. of the 19th EFTF, Besancon, France (2005).
- [2] G. Santarelli, Ph. Laurent, P. Lemonde, A. Clairon *Quantum Projection Noise in an Atomic Fountain : A High stability Cesium Frequency Standard*, Phys. Rev. Lett., vol 82, p 4619, (1999).
- [3] E. Simon, *Vers une stabilité et une exactitude de  $10^{-16}$  pour les horloges atomiques : - le rayonnement du corps noir - la détection optique*, Thesis from the Université Paris-XI, Orsay (1997).
- [4] S. Bize, *Tests fondamentaux l'aide d'horloges atomes froids de rubidium et de caesium*, Thesis from the Université Paris-VI, Paris (2001).
- [5] Y. Sortais, *Construction d'une fontaine double atomes froids de  $^{87}\text{Rb}$  et  $^{133}\text{Cs}$  ; étude des effets dépendant du nombre d'atomes dans une fontaine*, Thesis from the Université Paris-VI, Paris (2001).
- [6] G. Santarelli, C. Audoin, A. Makdissi, Ph. Laurent, G. Dick, A. Clairon *Frequency Stability Degradation of an Oscillator Slaved to a Periodically Interrogated Atomic Resonator*, IEEE Trans. Ultrason., Ferroelect., Freq. Contr., vol 45, p 887, (1998).
- [7] C. Audoin, G. Santarelli, A. Makdissi, A. Clairon *Properties of an Oscillator Slaved to a Periodically Interrogated Atomic Resonator*, IEEE Trans. Ultrason., Ferroelect., Freq. Contr., vol 45, p 877, (1998).
- [8] S. Tremine, S. Guerandel, D. Holleville, N. Dimarcq, A. Clairon, *Microwave interrogation in a compact atomic clock*, In Proc. of the 18th EFTF, Guilford, England (2004).
- [9] S. Tremine, S. Guerandel, D. Holleville, N. Dimarcq, A. Clairon, *Development of a compact cold atom clock*, In Proc. of the FCS, Montreal, Canada (2004).
- [10] P. Lemonde, Ph. Laurent, G. Santarelli, M. Abgrall, Y. Sortais, S. Bize, C. Nicolas, S. Zhang, A. Clairon, N. Dimarcq, P. Petit, A. Mann, A. Luiten, S. Chang, C. Salomon *Cold Atom Clocks on Earth and in Space*, Frequency Measurement and Control, Topics in Applied Physics, A. Luiten ed. 79, p 131, (2000).
- [11] P-E. Pottie, S. Trmine, S. Gurandel, N. Dimarck, A. Clairon, *3D speckle cooling in a microwave clock*, In Proc. of the 17th EFTF, Tampa, Florida (2003).